Diverse Range of Organic-Rich Cores in South Sea Non-Bead Cultured "Keshi" Pearls

Nishka Vaz, Abeer Al-Alawi, and Anukul Belanke

Known as South Sea "keshi" in the trade, these non-bead cultured pearls are byproducts of the bead culturing process within the *Pinctada maxima* mollusk, a source of both natural and cultured pearls. The internal features of some of these non-bead cultured pearls can pose a significant challenge in pearl identification due to their similarity to structures observed in natural pearls. A group of 43 pearls showing organic-rich concentric cores, reportedly sourced from an Australian pearl farm, was selected for this study. To determine origin, their structures were analyzed and categorized using several techniques, including real-time X-ray microradiography, computed microtomography, and energy-dispersive X-ray fluorescence chemical analysis. Five of the 43 pearls were partially sanded through their cores to allow for cross-sectional analysis, including visual observations and Raman spectroscopy, to correlate the structure and composition of these cores to their X-ray imagery. The results of this study will assist in separating non-bead cultured pearls formed inside the *Pinctada maxima* mollusk species from natural pearls from the same species.

South Sea cultured pearls, as they are commonly known in the trade, refer to pearls cultivated from the *Pinctada maxima* mollusk. These mollusks are renowned for producing some of the largest and most valuable cultured pearls (Otter et al., 2014; Smaal et al., 2019). Commercial culturing of these bivalves is carried out in the warm, nutrient-rich waters off the coasts of Australia, Myanmar, the Philippines, Indonesia, and in the South China Sea (Southgate and Lucas, 2008). Over the years, significant advances have been made in the methods and technology employed to produce high-quality cultured pearls, building upon the pearl culturing experiments initiated by Mikimoto in 1912 (Strack, 2001). Today, pearl farms produce non-bead cultured (NBC) pearls of large sizes and exceptional quality.

In the past, NBC pearls were mostly considered byproducts (Hänni, 2006); today, they are intentionally grown on pearl farms. Most NBC pearls are believed to grow in the gonad of the bivalves used for cultivating bead cultured pearls. Natural pearls, on the other hand, are known to form primarily in the mollusk's mantle. However, although most natural and cultured pearls have distinctly different internal structures, they also have similarities (Hänni, 2012). Hence, pearl testing laboratories must have adequate equipment and expertise to distinguish between natural and cultured pearls.

The internal structures of pearls are analyzed using real-time X-ray microradiography (RTX), and identification is based on recognizing features highlighted in

In Brief

- South Sea "keshi" pearls are byproducts with organic-rich cores featuring characteristics such as light gray nuclei, seed-like features, off-round nuclei, and multiple cores and/or nuclei.
- Cross sections of select samples exhibited similar structures in X-ray imaging with minor differences in appearance or texture of some nacre/organic-rich areas.
- Raman spectra of the cores' cross sections revealed aragonite as the dominant mineral phase with higher peak intensity in nacreous regions and lower intensity in more organic-rich areas. This correlated to the concentration of aragonite in these areas.

See end of article for About the Authors and Acknowledgments.
Gems & Gemology, Vol. 62, No. 1, pp. 26–37,
https://doi.org/10.5741/GEMS.62.1.26

previous research studies. The main structures observed in NBC pearls include voids, linear features, and organic-rich cores with loose ring structures and distinct seed features (Krzemnicki et al., 2010; Sturman et al., 2016; Nilpetploy et al., 2018; Homkrajae et al., 2021b). The radiopaque and radiolucent regions seen with X-rays result from variations in the composition of organic matrix and nacre (Rosc et al., 2016). While nacre itself consists of aragonite platelets cemented by organic phases, the latter material is a more chemically complex substance. The organic-rich matrix present in the internal structures of pearls that causes the darker areas to appear in X-ray imaging is composed of a combination of scleroproteins—which include amino acids such as leucine, alanine, glycerin, and cysteine—that are secreted by the mollusk (Tanaka et al., 1960). In this article, "organic-rich cores" refer to the dark and light gray concentric structures seen in the X-ray images of these pearls, while "nucleus" refers to their light gray centers. Technological advancements applied in pearl farming, along with environmental changes, have led to a gradual change in the internal structures observed in cultured pearls (Sturman et al., 2020). Therefore, it is important to routinely study the pearls originating from these farms.

MATERIALS AND METHODS

For this study, 43 nacreous NBC pearls from silver-lipped *Pinctada maxima* mollusks from Australia were selected (figure 1). These were acquired from a trusted dealer based in Mumbai who sources pearls directly from a farm in Australia. Only pearls with internal structures consisting of organic-rich cores

Figure 1. The 43 non-bead cultured "keshi" pearls (0.18 to 1.96 ct) from the Pinctada maxima *mollusk selected for this study. Photo by Gourav Bera.*

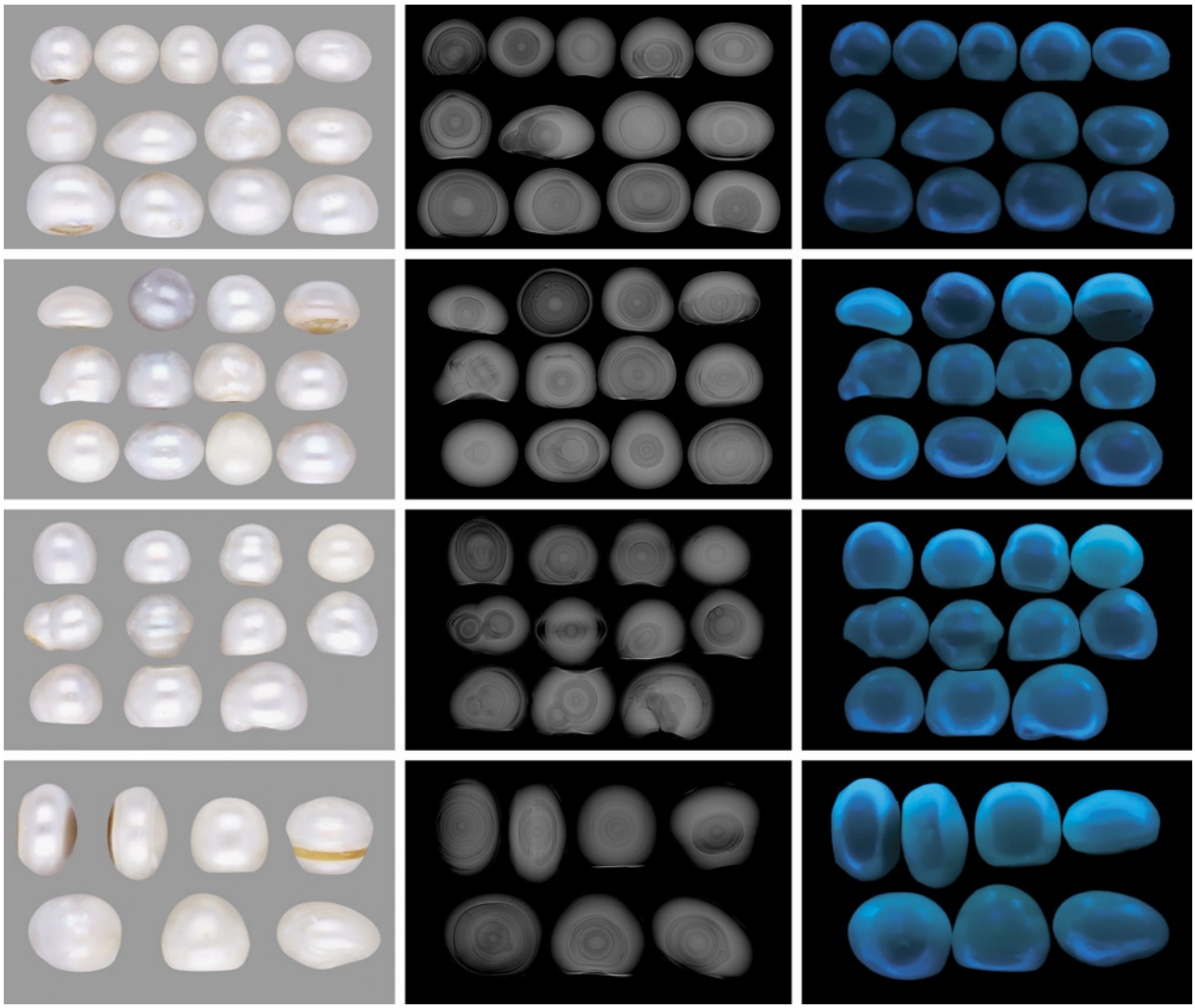

Figure 2. Photographs, RTX images, and long-wave UV reactions, respectively, of the 43 non-bead cultured pearls with organic-rich concentric cores from Pinctada maxima*, sorted by size. Photos by Gourav Bera.*

were selected through a preliminary evaluation by RTX imaging (figure 2). The majority of these pearls were button shaped with flat or concave surfaces on one side forming a base, with a few near-drop and baroque-shaped pearls. They ranged from 3.37 × 3.15 × 2.92 mm to 7.69 × 7.33 × 5.23 mm in size and weighed 0.18 to 1.96 ct. Among the 43 examined pearls, three ranged from light gray to gray, three displayed a silver hue, and the remaining 37 were white in color. Most of the pearls exhibited orient.

The internal structures of these samples were further categorized into four subgroups, with four pearls selected from each group as representative examples based on the radiopacity and pattern of features they showed in RTX and X-ray computed microtomography (μ-CT) imagery. These pearls were assigned sample identifiers based on their structural classification:

- Group A: Core with a light gray nucleus (pearls A-1 through A-4)
- Group B: Seed-like features (pearls B-1 through B-4)
- Group C: Off-round core and nuclei (pearls C-1 through C-4)
- Group D: Multiple cores and/or nuclei (pearls D-1 through D-4)

To further study their composition, five of the 43 pearls with internal structures representing each group (one each from groups A–C and two from group D) were sanded down to their cores. Raman spectroscopy was also performed on multiple spots

along the cross sections for an overview of the compositions of these areas.

All the samples were examined using a binocular gemological microscope under magnifications of 10× to 135× with fiber-optic illumination. The reactions of all samples were studied under various radiations: X-ray fluorescence using a FocalSpot Verifier FSX-PF100 unit with 100 kV voltage, and 5 mA current X-ray source and a GIA-designed UV unit incorporating a narrowband 365 nm long-wave ultraviolet and 254 nm short-wave ultraviolet LED source.

RTX was performed on all samples using a Pacific X-ray Imaging GenX 90P X-ray inspection system with a 4 μm microfocus, 90 kV voltage, and a 0.150 mA current X-ray source with an exposure time of 200–400 milliseconds per frame combined with a PerkinElmer 1512 flat panel detector with a maximum of 128 frames average and 74.8 micropixel pitch with 1920 × 1080 pixel resolution. X-ray computed microtomography was also performed for all 43 pearl samples using a ProCon CT-MINI X-ray system with a 5 μm microfocus, 130 kV voltage, and 0.30 mA current X-ray source with a Varex 1207 flat panel detector with 74.8 micropixel pitch and 1944 × 1536 pixel resolution. Raman spectra were obtained using a Renishaw inVia micro-Raman spectrometer system with a 50× magnification Leica objective lens and an 830 nm diode laser. This laser provided a better resolution of mineral peaks than the 514 nm laser often used for Raman spectroscopy of pearls. A laser power of 50 mW was used directly on the samples, and the system was calibrated with a silicon standard. The elastic Rayleigh scattering was blocked using edge filters. The laser was set at 50–100% power with three accumulations and an exposure time of 10 seconds with a grating of 1200 grooves/mm.

Chemical analyses were conducted on all the samples using an energy-dispersive X-ray fluorescence (EDXRF) spectrometer and a Thermo Scientific ARL QUANT'X system calibrated using U.S. Geological Survey (USGS) carbonate microanalytical reference materials MACS-1 and MACS-3 (in pressed powder pellet form), incorporating a 50 W, 4–50 kV voltage, and 0.02–1.98 mA current X-ray source with a SDD500G silicon-lithium drifted detector.

OBSERVATIONS AND DISCUSSION

External Observations. Each pearl sample exhibited a smooth surface with lustrous appearance. Under high magnification, fine, evenly spaced overlapping nacreous terrace structures were visible, some with a spiral pattern typical of pearls from *Pinctada maxima* (figure 3A). Most of the button-shaped pearls had

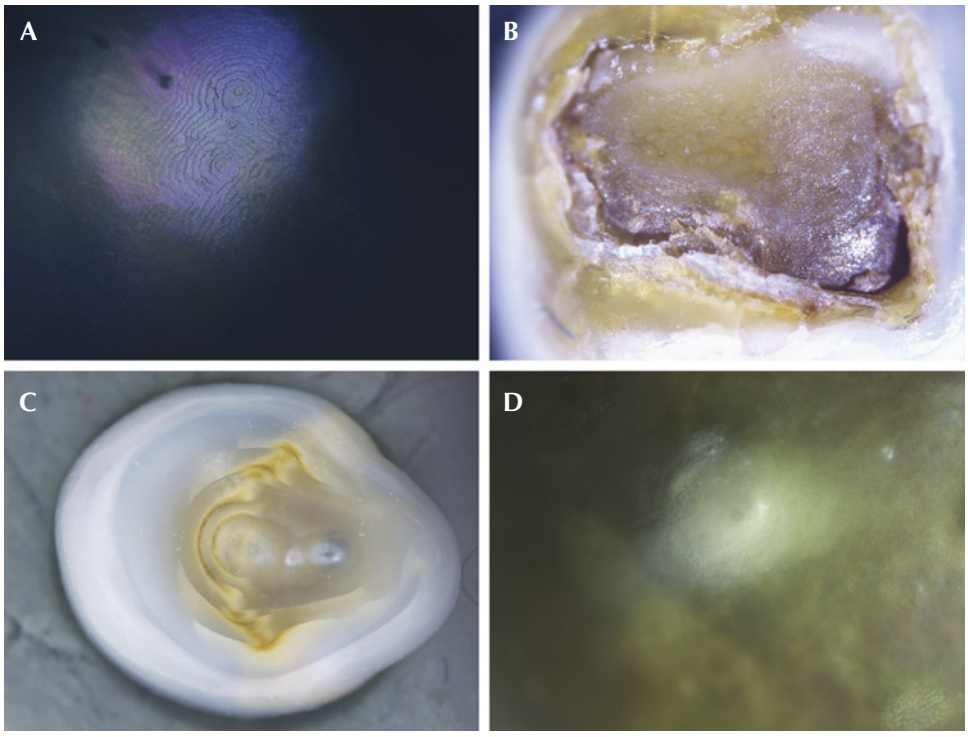

Figure 3. A: A spiral nacreous terrace structure on pearl A-2. B: The base of pearl C-4 with uneven organic-rich layers. C: Concave base on pearl D-4 with cores and nuclei seen through translucent nacre. D: Subsurface white spots on pearl B-1. Photomicrographs by Nishka Vaz; fields of view 0.5 mm (A), 1.3 mm (B), 3.2 mm (C), and 0.85 mm (D).

organic-rich patches evident on the bases. In addition, areas of broken nacre with darker brown and lighter translucent organic-rich layers interspersed with nacre layers were commonly found on the pearls' bases (figure 3B). Button-shaped pearls with concave bases and visible growth arcs with the cores occasionally apparent are also typical features associated with NBC pearls. These could also have a double core with bulging areas due to the accumulation of organic-rich material seen in the growth arcs (figure 3C). Moreover, translucent surface nacre can reveal features such as the white bumps associated with NBC pearls (figure 3D), which may be either subsurface or raised. Although white spots in freshwater cultured pearls are associated with the presence of vaterite (Wehrmeister et al., 2007), the pearls studied did not appear to contain vaterite based upon their Raman spectra.

All the pearls showed an inert reaction when exposed to X-ray fluorescence (XRF), indicating saltwater origin. EDXRF analysis conducted on all pearls revealed manganese levels ranging from below detection limit (29.8 ppmw) to 39.8 ppmw and strontium levels ranging from 1403 to 3301 ppmw. These levels are a good indicator of the marine environment in which the pearls formed and are comparable to those observed in pearls from the *Pinctada maxima* mollusk (Karampelas et al., 2019b).

With exposure to long-wave UV, a near-uniform moderate blue fluorescence reaction was observed on all of the pearls' surfaces. In addition, short-wave UV exposure gave a similar but weaker blue fluorescence reaction.

Internal Structures. Because pearls are organic gems formed through biological processes within a mollusk (Vaz et al., 2023), each pearl possesses some unique characteristics. Although it is not always easy to distinguish between natural and cultured pearls (Sturman et al., 2019; Homkrajae et al., 2021a), certain textures and patterns in their internal structures can help indicate whether human influence led to the pearl's formation. Examining these types of structures in pearls of reported NBC origin aids laboratories in providing accurate results for the pearls submitted for testing.

All the selected pearls revealed cores with different forms of organic-rich concentric structures (again, see figure 2). Both natural and cultured pearls from *Pinctada maxima* often have cores with distinct organic-rich concentric structures (Scarratt et al., 2012; Manustrong et al., 2019); hence, it is important to study the differences in the structures of such cores from natural and cultured pearls. Four types of internal structures were observed in the studied pearls.

Group A: Core with a Light Gray Nucleus. The centers of the large organic-rich concentric cores observed in NBC pearls are often composed of a calcium carbonate ($CaCO_3$) nucleus that appears light gray in RTX and μ-CT imagery. This nucleus indicates the initiation point of the pearl's growth. Thus, layers formed around the nucleus progressively decrease in age from the point of initiation, with the outermost layers formed most recently. The nucleus may vary in size, as observed in the samples in table 1. A distinct boundary is often visible between the core and the alternating light and dark rings of nacre and organic-rich material, respectively. In some pearls, such as A-1, the dark organic-rich core exhibits very faint patchiness in addition to the concentric pattern, whereas other pearls, such as A-2, may display well-defined fine rings of nacre within the organic-rich

TABLE 1. Group A: Four non-bead cultured pearls from *Pinctada maxima* with light gray nuclei and core structures (red arrow indicates step-down features).

Sample	Macro	RTX	μ-CT
A-1 0.22 ct 3.26 × 3.21 × 3.14 mm	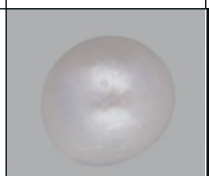		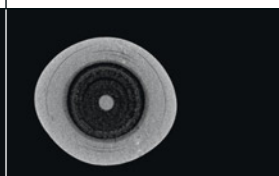
A-2 0.80 ct 5.25 × 5.24 × 4.98 mm			
A-3 0.56 ct 5.13 × 5.11 × 3.53 mm			
A-4 0.31 ct 4.03 × 3.99 × 2.72 mm	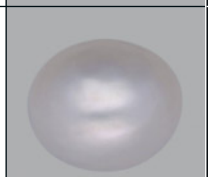		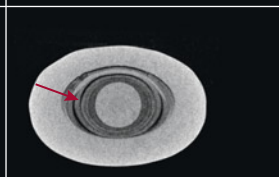

concentric core. A dark radiolucent ring may also be observed around the circumference of the pearl. When viewed in μ-CT, it appears as a bulge of organic-rich material on either side of the core, such as in pearl A-2.

Another pattern for the more radiolucent alternating layers may also be seen. The thickness and tightness of these rings and their textures are important details to note in such cores. While distinct uniformly thick rings are more frequently seen in cultured pearls, radiolucent crescent-shaped gaps between consecutive layers, known as "loose layers," may also be present. On some occasions, these loose layers can appear as though a single concentric layer is flowing from one level to the next, producing a "step down" feature as observed in pearls A-3 and A-4 (indicated with arrow), and has been often observed in South Sea NBC pearls (Homkrajae et al., 2021b). Additionally, a faint acicular pattern can also be seen radiating from the nucleus in the central region of the core, such as that in A-3. A common observation in cultured pearls is the presence of a thick layer of nacre growth around the core that lacks growth arcs, such as that in pearl A-4. This lack of growth arcs has been speculatively attributed to the rapid growth of nacre in cultured pearls (Scarratt et al., 2017). The large round nuclei seen in pearl A-4 and the lack of structure within the nuclei are more commonly observed in NBC pearls rather than in natural ones, especially in pearls from the *Pinctada maxima* mollusk. Similarly, the presence of cracks running through the core or radiating within the organic-rich layers, potentially due to the pearl's desiccation, was evident in pearls A-2 and A-3.

Group B: Seed-Like Features. In addition to the nucleus, similar light gray concretions indicative of the calcium carbonate matrix are also often found within the organic-rich layers. When these concretions occur beyond the point of initiation (nucleus), they are often referred to as "seed" features or "globuli" (light gray features shown in the organic-rich concentric cores in pearls in table 2). The sizes of these seed features vary significantly, with some appearing larger than the nucleus, equivalent to it in size, or much smaller, such as in pearls B-2, B-3, and B-4, respectively. Unlike the nucleus, these seeds are always found after the initiation of the pearl, during its growth. As these features are composed of nacre and potentially form during the deposition of the organic-rich matrix, the concentric layers of the core often deform as they flow around these concretions.

TABLE 2. Group B: Four non-bead cultured pearls from *Pinctada maxima* with seed-like features.

Sample	Macro	RTX	μ-CT
B-1 0.46 ct 4.88 × 4.54 × 4.51 mm	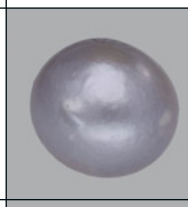	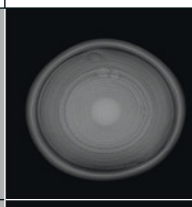	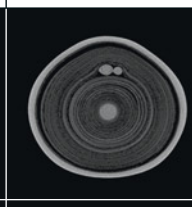
B-2 0.65 ct 4.85 × 4.44 × 4.37 mm		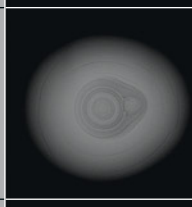	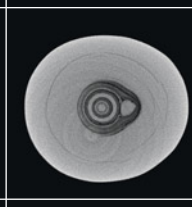
B-3 0.30 ct 3.72 × 3.65 × 3.11 mm	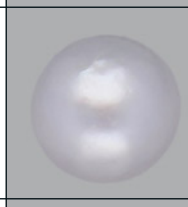	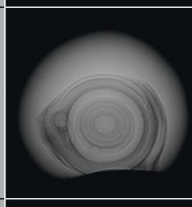	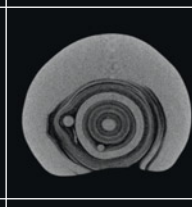
B-4 0.88 ct 5.40 × 5.03 × 4.79 mm	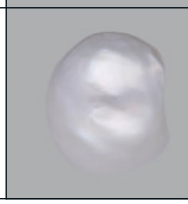	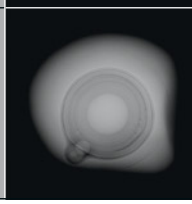	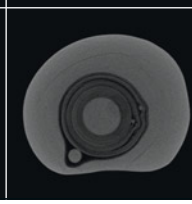

In cultured pearls, these seeds are often embedded in the layers of the organic-rich concentric core. Although most seed features are round and light gray, it is not uncommon to find seeds with minor growth features such as growth arcs or slightly elongated seeds, as in pearls B-1 and B-2. Often, these seeds or globuli are not easily visible in RTX but are clearly seen in μ-CT images, such as in pearl A-2. Hence, laboratories exercise extreme caution while testing pearls with such cores. The presence of a thick light gray ring within these concentric layers, as seen in pearls B-2 and B-3, is also commonly observed in NBC pearls from *Pinctada maxima*.

Group C: Off-Round Cores and Nuclei. Off-round cores and nuclei (table 3) are considered characteristic features of South Sea NBC pearls (Manustrong et al., 2019). Although natural pearls may occasionally have nuclei that are not perfectly round, the presence of a distinctly oval-, pear-, or lens-shaped calcium carbonate nucleus within a pearl is likely a result of the culturing process. Off-round cores with oval nuclei, such as those seen in pearls C-1 and C-2, are

TABLE 3. Group C: Four non-bead cultured pearls from *Pinctada maxima* with off-round cores and nuclei.

Sample	Macro	RTX	μ-CT
C-1 1.96 ct 6.92 × 6.69 × 5.96 mm			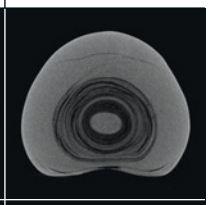
C-2 0.86 ct 5.15 × 5.08 × 4.39 mm			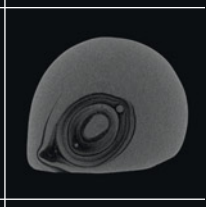
C-3 0.73 ct 4.84 × 4.80 × 4.69 mm		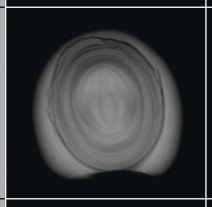	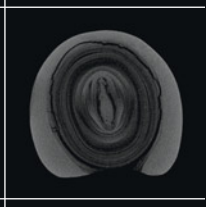
C-4 0.18 ct 3.37 × 3.15 × 2.92 mm		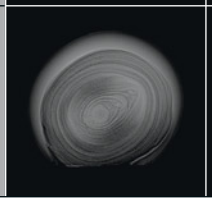	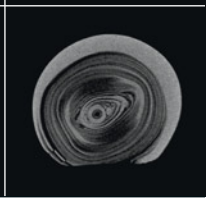

examples of such structures. Despite their relatively dense, radiopaque nature, these nuclei seem to be enclosed in a radiolucent organic-rich layer. Unlike the light gray nuclei in group A, these off-round nuclei often exhibit minimal faint growth arcs. More extreme versions of these distorted nuclei were observed in pearls C-3 and C-4, where the nuclei have a highly elongated spindle shape with the pointed edges curving in on the elongated nucleus in pearl C-3, and where a complex elliptical nucleus has multiple nuclei or seeds attached to it, as in pearl C-4. Notably, the shape of the core itself appears independent of the central nucleus. This inconsistency in shape from nucleus to core to the shape of the pearl itself is observed more in NBC pearls, which is reflected in the 43 pearls studied. This is obvious in pearl C-1, where the nucleus appears oval in a round organic-rich concentric area that grows into a button-shaped core and pearl. Similarly, the oval nucleus in pearl C-2 is also surrounded by oval organic-rich concentric layers that are further distorted by two seeds present at alternating axial positions. A radiolucent dark gray pocket outside the core is also an observed feature often associated with bead cultured pearls due to the culturing process (Krzemnicki et al., 2010), which might be seen in NBC pearls as well. A gradual change in the pearl's shape from nucleus to nacre due to the shape of the organic-rich layers of the core can be seen in C-3 and C-4, with the denser light gray rings evident along axial positions and the looser, darker rings visible along the sides.

Group D: Multiple Cores and/or Nuclei. While multiple cores are occasionally observed in natural pearls, they are more prevalent in NBC pearls. For instance, pearl D-1 in table 4 features a large core adjacent to two smaller cores in contact with each other. The larger feature (main core) contains a light gray calcium carbonate nucleus surrounded by loose organic-rich layers and a distinct thick, large light gray ring, a characteristic not typically observed in natural pearls from the same species. The organic-rich layers surrounding this core exhibited multiple step-down features. Conversely, the other two smaller cores are enfolded by a dense organic layer that appears to have an acicular radial texture following the outline of the two cores. The multiple cores may further be enveloped by layers of an organic-rich concentric structure as seen in pearls D-2 and D-3 and may be either of different sizes and shapes, as in pearl D-2, or similar sizes but different textures, as seen in pearl D-3. The structure of these two pearls is also a good example of the differences between various types of organic-rich concentric structures. While the radiopacity of the rings in pearl D-2 is darker and more contrasted compared to the more diffused concentric layers of pearl D-3, they both show loose structures, step-down features, and voids between the cores. A more complex structure can be seen in pearl D-4, where the pearl contains four nuclei, three of which appear as dense light gray calcium carbonate entities, while one appears to have some organic structure around it. Three of the nuclei are in contact with one another and surrounded by a series of organic-rich layers and significant cracks that fuse into the nacre at one end, with one nucleus surrounded by nacre outside these layers. Natural pearls may occasionally show structures with multiple cores and/or nuclei (Homkrajae et al., 2021a); however, their patterns and arrangements are distinctly different from those seen in cultured pearls. Based on GIA's observations of numerous pearls from both known samples and client submissions, such cores are considered type examples for NBC pearls.

TABLE 4. Group D: Four non-bead cultured pearls from *Pinctada maxima* with multiple cores and/or nuclei.

Sample	Macro	RTX	μ-CT
D-1 0.78 ct 6.11 × 4.57 × 4.36 mm	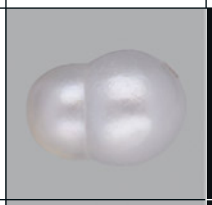		
D-2 1.23 ct 6.18 × 5.65 × 4.70 mm		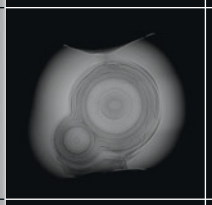	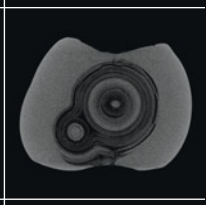
D-3 0.91 ct 5.65 × 5.10 × 4.62 mm		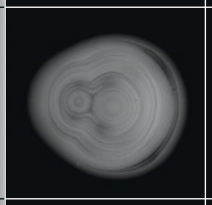	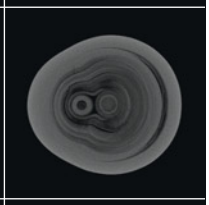
D-4 0.61 ct 5.43 × 4.40 × 3.99 mm	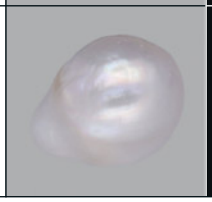	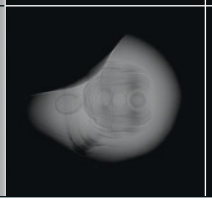	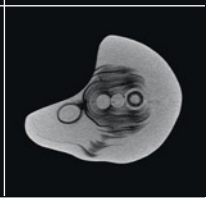

Raman Spectroscopy. Pearl identification in laboratories is carried out by studying internal structures through nondestructive tests such as RTX and μ-CT. However, it is also important to visualize the pearl's internal structure and understand its composition; therefore, five pearl samples were sanded down to their cores to further analyze their cross sections.

Raman spectra collected with an 830 nm laser helped identify three distinct phases based on the composition of the material at different points of the core. The nacre and light regions showed distinct peaks at 1086 cm^{-1}, a doublet or broad peak at 701/705 cm^{-1}, and a series of peaks from 100 to 280 cm^{-1}. These peaks indicate the presence of an aragonite mineral phase. In addition to these peaks, a few spots on the surface showed a small peak around 716 cm^{-1}, indicating the presence of magnesium-rich calcite along with aragonite peaks, showing a bimineralic composition in these areas. While the calcite Raman peak in pearls is typically observed at 712 cm^{-1}, this shift has previously been attributed to vibrational modes at longer wavelengths and the presence of higher magnesium content in calcite (Sun et al., 2014; Borromeo et al., 2017; Karampelas et al., 2019a). Very weak or no mineral peaks were observed in the organic-rich areas due to high concentrations of organic matter rather than mineral-rich phases.

The cross section of pearl A-4 showed similarities to its RTX and μ-CT images outlined in table 1. These similarities are evident in the radiopacity of the nuclei and nacre with X-ray imaging, which also appear more solid and white along the cross section. Furthermore, the organic-rich concentric core around the nucleus also displays a pattern similar to that observed with X-rays, with the darker areas appearing more organic-rich and the lighter areas more aragonite-rich, based on the relative intensity of the aragonite peaks as seen in the Raman spectra (figure 4).

Figure 4. Left: Cross section of pearl A-4 with spots marked for Raman spectroscopy. Photo by Nishka Vaz; field of view 2.7 mm. Right: Raman spectra collected with an 830 nm laser from pearl A-4 on indicated spots, showing peaks of varying intensity at 1086 cm^{-1}, 701/705 cm^{-1}, and 100–280 cm^{-1}, indicating the presence of aragonite. Spectra are baseline corrected and offset vertically for clarity.

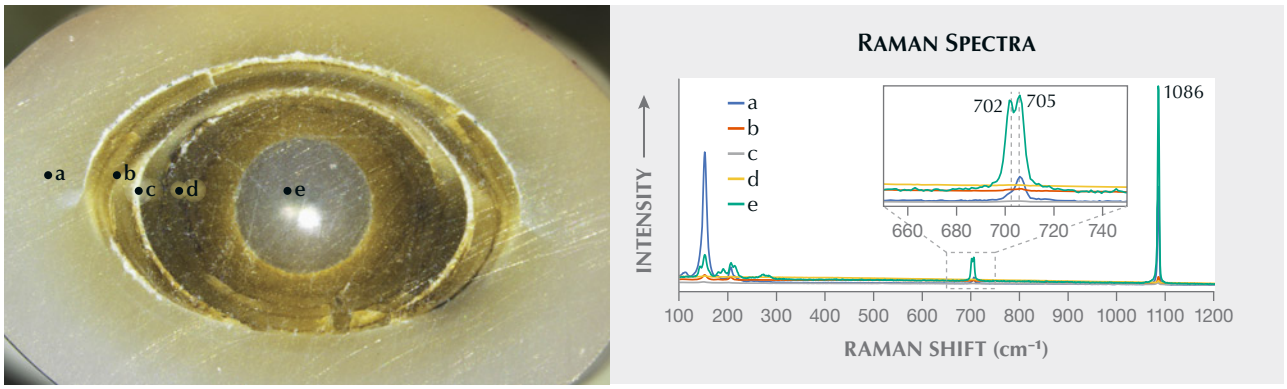

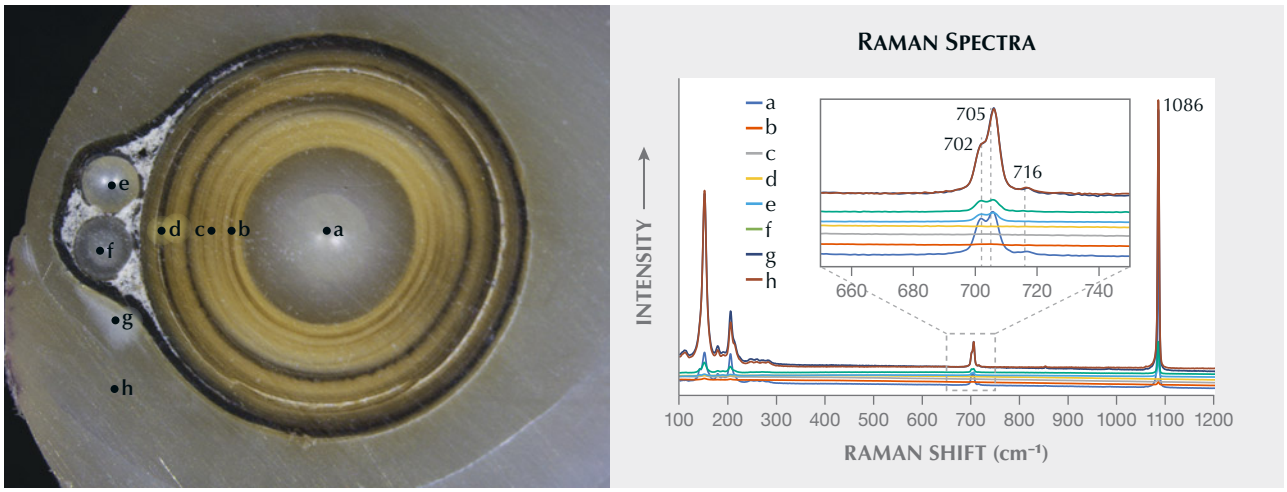

Figure 5. Left: Cross section of pearl B-4 with spots marked for Raman spectroscopy. Photo by Nishka Vaz; field of view 3.19 mm. Right: Raman spectra collected with an 830 nm laser from pearl B-4 on indicated spots, showing peaks of varying intensity at 1086 cm^{-1}, 701/705 cm^{-1}, and 100–280 cm^{-1}, indicating the presence of aragonite. Spots a, g, and h showed an additional weak peak at 716 cm^{-1}, indicating a calcite phase in addition to aragonite, while spot d showed very weak mineral peaks due to higher organic content in those regions. Spectra are baseline corrected and offset vertically for clarity.

Similarly, the cross section of pearl B-4 also resembled its RTX and μ-CT images (again, see table 2), with the large light gray core appearing similar to that seen in pearl A-4. However, unlike the similarities in radiopacity seen in the X-ray images, the organic-rich concentric core appears much lighter in pearl B-4. Additionally, the nucleus and surrounding nacre of the pearl also showed the presence of very weak calcite peaks in Raman spectroscopy in addition to aragonite, indicating a likely bimineralic composition dominated by aragonite with minor calcite (figure 5).

The cross section of pearl C-3, with its spindle-shaped nucleus, revealed an interesting structure. This nucleus appeared to be light colored, with the organic-rich concentric structure surrounding it matching the pattern seen in the X-ray images (again, see table 3). A distinctive difference between the two stages of growth in the organic-rich core was also visible. The initial stage after the formation of the nucleus appears to be followed by a series of mineral-dominant rings around the nucleus, succeeded by a stage of growth of organic-rich dominant concentric layers. This distinction can be observed in the radiopacity of the layers corresponding to their color when sanded into cross sections and in the intensity of the aragonite peaks seen in Raman spectra. A dense layer of nacre deposition appears to have occurred after the core formation, and both the nacre and the core are composed of aragonite based on their Raman spectra (figure 6).

Pearl D-1 was sanded down to reveal its triplet cores. As observed in the μ-CT images, all three of these cores had distinctly different structures (again, see table 4). From the point of initiation to the radiopacity to the texture of the organic-rich layers around them, all three of these cores and the organic-rich layer enveloping the two smaller cores differed in pattern and appearance. This variance likely signifies the individual growth of each nucleus in different pearl sacs within the mollusk, ultimately fusing together to form an aggregate pearl (Mariom et al., 2019). The compositions of these cores also had varying aragonite content, as seen from the intensity of their corresponding peaks in the Raman spectra. The white ring in the larger core, often associated with NBC pearls from *Pinctada maxima*, as well as the pearl nacre were composed of a bimineralic phase with faint calcite peaks in addition to strong aragonite Raman peaks. The void-like areas between the cores observed in both the RTX and μ-CT images appeared to be filled with a resinous organic material that did not exhibit strong mineral peaks due to its organic-rich composition (figure 7).

The complex arrangement of nuclei and cores in pearl D-4 also proved to be an intriguing study. Unlike the multiple cores in pearl D-1, this structure appears to be an aggregate of nuclei comprising of round/oval bodies in spots f, h, and k, as well as small

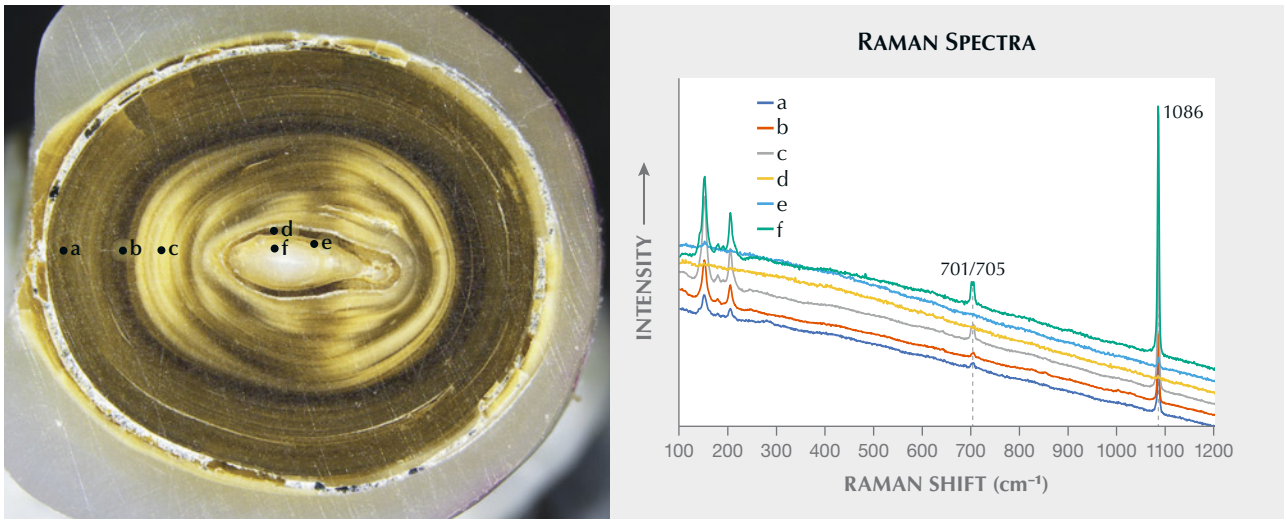

Figure 6. Left: Cross section of pearl C-3 with spots marked for Raman spectroscopy. Photo by Nishka Vaz; field of view 6.8 mm. Right: Raman spectra collected with an 830 nm laser from pearl C-3 on indicated spots, showing peaks of varying intensity at 1086 cm^{-1}, 701/705 cm^{-1}, and 100–280 cm^{-1}, indicating the presence of aragonite. Spots a, c, and f showed weak to moderate aragonite peaks, while spots b, d, and e appeared to be more organic-rich, with very weak to almost absent mineral peaks at spot d. Due to the relatively higher organic content of these spots, the baseline appears to be raised toward the lower Raman shift end. Spectra are baseline corrected and offset vertically for clarity.

round cores, as seen in spots d and j (figure 8). These cores and aggregates are surrounded by organic-rich layers and nacre with a small seed observed at spot n. Although the darker areas of this pearl are more organic-rich based on the Raman spectra, and aragonite seems to be the dominant mineral phase in the nacreous regions, the outer nacre and nucleus at spot h seem to have weak calcite peaks, indicating a bimineralic phase dominated by aragonite with minor calcite in these regions.

Figure 7. Left: Cross section of pearl D-1 with spots marked for Raman spectroscopy. Photo by Nishka Vaz; field of view 4.5 mm. Right: Raman spectra collected with an 830 nm laser from pearl D-1 on indicated spots, showing peaks of varying intensity at 1086 cm^{-1}, 701/705 cm^{-1}, and 100–280 cm^{-1}, indicating the presence of aragonite. Spots a and i showed an additional weak peak at 716 cm^{-1}, indicating a calcite phase in addition to aragonite, while spots b, j, and k showed very weak mineral peaks due to higher organic content in those regions. Spectra are baseline corrected and offset vertically for clarity.

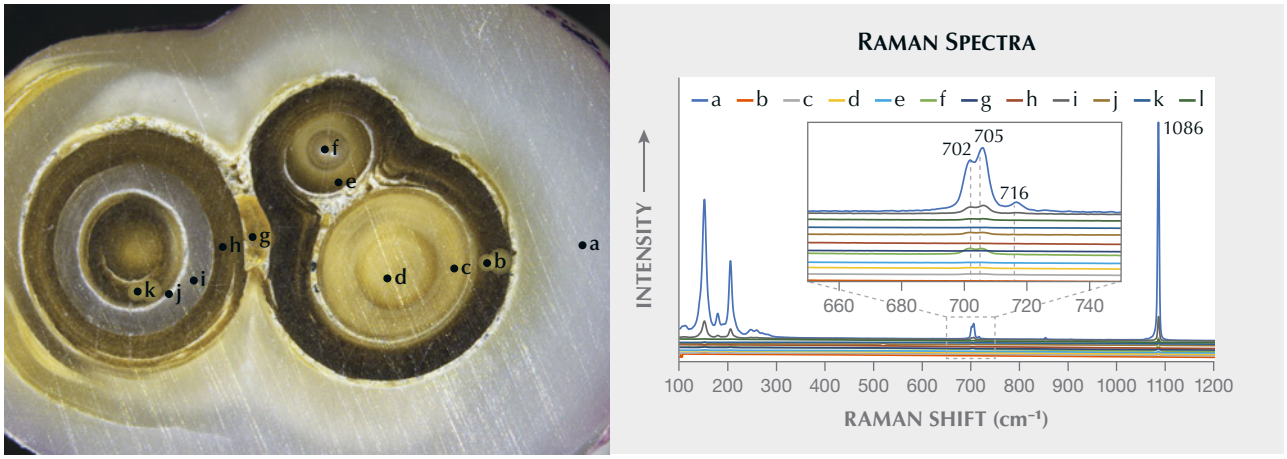

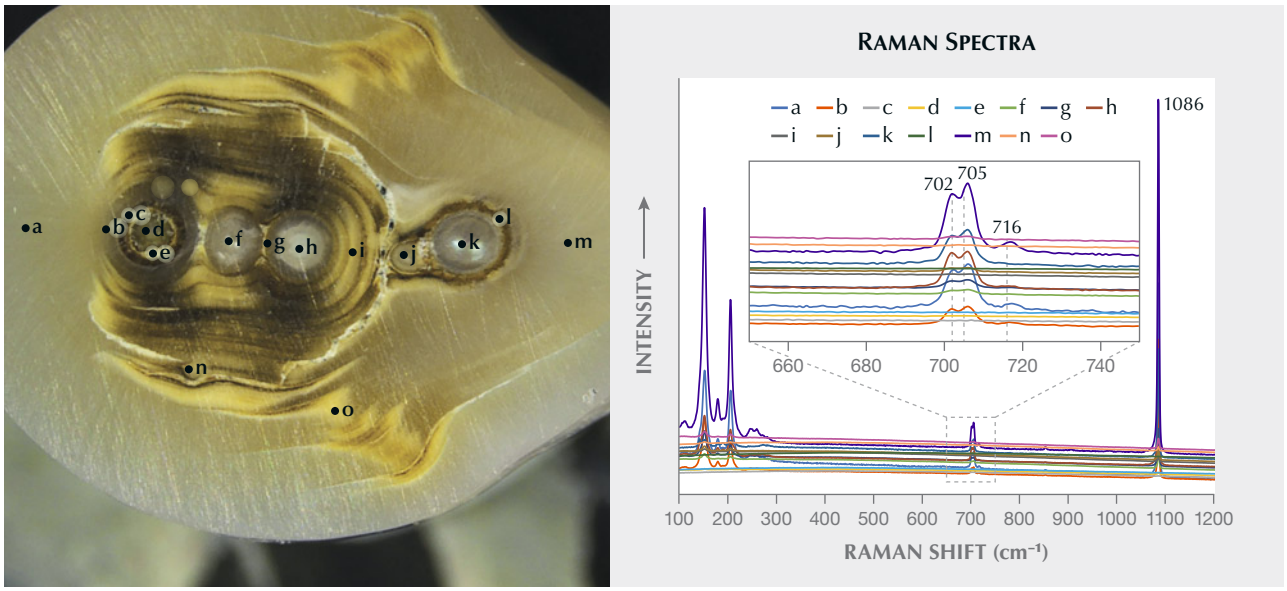

Figure 8. Left: Cross section of pearl D-4 with spots marked for Raman spectroscopy. Photo by Nishka Vaz; field of view 4.5 mm. Right: Raman spectra collected with an 830 nm laser from pearl D-4 on indicated spots, showing peaks of varying intensity at 1086 cm^{-1}, 701/705 cm^{-1}, and 100–280 cm^{-1}, indicating the presence of aragonite. Spots a, b, g, h, and m showed an additional weak peak at 716 cm^{-1}, indicating a calcite phase in addition to aragonite. Spectra are baseline corrected and offset vertically for clarity.

CONCLUSION

NBC pearls from the *Pinctada maxima* mollusk tend to have a distinct appearance compared to those from most natural and cultured pearls from other *Pinctada* species. Their silky luster and often large sizes distinguish them from other pearls. While this mollusk is a source of both natural and cultured pearls, certain features are more often seen in cultured pearls, such as the texture and pattern of terrace structures formed by aragonite platelets in the nacre, concave bases with resinous patches of organic-rich material often exhibiting desiccation fissures, and small white subsurface spots from underlying seeds. These external features are helpful indicators to support other data used to identify a pearl's origin.

The internal structure seen in microradiographs can also provide valuable insights about the identity of a pearl. Certain features such as the texture of the rings in organic-rich concentric cores, the presence of a distinct calcium carbonate nucleus, seeds or globuli within the organic-rich concentric core, multiple cores and/or nuclei features, and off-round nuclei are strong indicators of NBC pearls from *Pinctada maxima*. Additionally, supporting features such as white rings, step-down features, loose structures, desiccation fissures, distinct alternating light and dark rings, and very dark and patchy acicular radial cores are often considered signs that support an NBC origin.

It is noteworthy that the cores in the selected groups chosen for cross-sectional analysis exhibited similar structures in X-ray imaging and in cross section, with minor differences in appearance or texture of some areas of nacre or organic-rich regions. However, all the cores in the pearls studied seemed to contain a combination of organic-rich phases and calcium carbonate mineral phases, with a few pearls showing very weak calcite peaks in addition to strong aragonite peaks in the nacreous regions.

Whether natural or non-bead cultured, each organic-rich concentric core is unique. The factors discussed in this article represent only a few of the numerous features that must be considered while testing pearls. These structures encompass typical features that are representative of cores observed in many of the South Sea NBC pearls in circulation today.

ABOUT THE AUTHORS
Nishka Vaz is a senior gemologist, and Anukul Belanke is an analytics technician, at GIA in Mumbai. Abeer Al-Alawi is a consultant to GIA.

ACKNOWLEDGMENTS
The authors thank Milan Jhaveri and Karnil Jhaveri for their help with sourcing the pearls studied in this article.

REFERENCES

Borromeo L., Zimmermann U., Andò S., Coletti G., Bersani D., Basso D., Gentile P., Schulz B., Garzanti E. (2017) Raman spectroscopy as a tool for magnesium estimation in Mg-calcite. *Journal of Raman Spectroscopy*, Vol. 48, No. 7, pp. 983–992, https://doi.org/10.1002/jrs.5156

Hänni H.A. (2006) A short review of the use of 'keshi' as a term to describe pearls. *Journal of Gemmology*, Vol. 30, No. 9, pp. 51–58.

——— (2012) Natural pearls and cultured pearls: A basic concept and its variations. *Australian Gemmologist*, Vol. 24, No. 11, pp. 258–266.

Homkrajae A., Manustrong A., Nilpetploy N., Sturman N., Lawanwong K., Kessrapong P. (2021a) Internal structures of known *Pinctada maxima* pearls: Natural pearls from wild marine mollusks. *G&G*, Vol. 57, No. 1, pp. 2–21, https://doi.org/10.5741/GEMS.57.1.2

Homkrajae A., Nilpetploy N., Manustrong A., Sturman N., Lawanwong K., Kessrapong P. (2021b) Internal structures of known *Pinctada maxima* pearls: Cultured pearls from operated marine mollusks. *G&G*, Vol. 57, No. 3, pp. 186–205, https://doi.org/10.5741/GEMS.57.3.186

Karampelas S., Fritsch E., Makhlooq F., Mohamed F., Al-Alawi A. (2019a) Raman spectroscopy of natural and cultured pearls and pearl-producing molluscs. *Journal of Raman Spectroscopy*, Vol. 51, No. 9, pp. 1813–1821, https://doi.org/10.1002/jrs.5670

Karampelas S., Mohamed F., Abdulla H., Almahmood F., Flamarzi L., Sangsawong S., Al-Alawi A. (2019b) Chemical characteristics of freshwater and saltwater natural and cultured pearls from different bivalves. *Minerals*, Vol. 9, No. 6, article no. 357, https://doi.org/10.3390/min9060357

Krzemnicki M.S., Friess S.D., Chalus P., Hänni H.A., Karampelas S. (2010) X-ray computed microtomography: Distinguishing natural pearls from beaded and non-beaded cultured pearls. *G&G*, Vol. 46, No. 2, pp. 128–134, https://doi.org/10.5741/GEMS.46.2.128

Manustrong A., Kessrapong P., Lawanwong K., Nilpetploy N., Homkrajae A. (2019) Known non-nacreous non-bead cultured pearls and similar unknown pearls of likely cultured origin from *Pinctada maxima*. *GIA Research News*, September 4, https://www.gia.edu/gia-news-research/known-non-nacreous-non-bead-cultured-pearls

Mariom T., Take S., Igarashi Y., Yoshitake K., Asakawa S., Maeyama K., Nagai K., Watabe S., Kinoshita S. (2019) Gene expression profiles at different stages for formation of pearl sac and pearl in the pearl oyster *Pinctada fucata*. *BMC Genomics*, Vol. 20, No. 1, article no. 240, https://doi.org/10.1186/s12864-019-5579-3

Nilpetploy N., Lawanwong K., Kessrapong P. (2018) Non-bead-cultured pearls from *Pinctada margaritifera*, *GIA Research News*, April 27, https://www.gia.edu/gia-news-research/non-bead-cultured-pearls-from-pinctada-margaritifera

Otter L.M., Wehrmeister U., Enzmann F., Wolf M., Jacob D.E. (2014) A look inside a remarkably large beaded South Sea cultured pearl. *G&G*, Vol. 50, No. 1, pp. 58–62, https://doi.org/10.5741/GEMS.50.1.58

Rosc J., Hammer V.M.F., Brunner R. (2016) X-ray computed tomography for fast and non-destructive multiple pearl inspection. *Case Studies in Nondestructive Testing and Evaluation*, Vol. 6, Part A, pp. 32–37, https://doi.org/10.1016/j.csndt.2016.08.002

Scarratt K., Bracher P., Bracher M., Attawi A., Saeseaw S., Homkrajae A., Sturman N. (2012) Natural pearls from Australian *Pinctada maxima*. *G&G*, Vol. 48, No. 4, pp. 236–261, https://doi.org/10.5741/GEMS.48.4.236

Scarratt K., Sturman N., Tawfeeq A., Bracher P., Bracher M., Homkrajae A., Manustrong A., Somsa-Ard N., Zhou C. (2017) Atypical "beading" in the production of cultured pearls from Australian *Pinctada maxima*. *GIA Research News*, February 13, https://www.gia.edu/gia-news-research/atypical-beading-production-cultured-pearls-australian-pinctada-maxima

Smaal A.C., Ferreira J.G., Grant J., Petersen J.K., Strand Ø. (2019) *Goods and Services of Marine Bivalves*. Springer, Berlin, https://doi.org/10.1007/978-3-319-96776-9

Southgate P.C., Lucas J.S. (2008) *The Pearl Oyster*. Elsevier, Oxford, UK, https://doi.org/10.1016/b978-0-444-52976-3.x0001-0

Strack E. (2001) *Pearls*. Ruhle-Diebener-Verlag, Stuttgart, Germany.

Sturman N., Bergman J., Poli J., Homkrajae A., Manustrong A., Somsa-ard N. (2016) Bead-cultured and non-bead-cultured pearls from Lombok, Indonesia. *G&G*, Vol. 52, No. 3, pp. 288–297, https://doi.org/10.5741/GEMS.52.3.288

Sturman N., Otter L.M., Homkrajae A., Manustrong A., Nilpetploy N., Lawanwong K., Kessrapong P., Jochum K.P., Stoll B., Götz H., Jacob D.E. (2019) A pearl identification challenge. *G&G*, Vol. 55, No. 2, pp. 229–243, https://doi.org/10.5741/GEMS.55.2.229

Sturman N., Lawanwong K., Kitdee N., Chodhri D. (2020) Vietnam: Shell nuclei, pearl hatcheries, and pearl farming. *G&G*, Vol. 56, No. 3, pp. 402–415, https://doi.org/10.5741/GEMS.56.3.402

Sun J., Wu Z., Cheng H., Zhang Z., Frost R.L. (2014) A Raman spectroscopic comparison of calcite and dolomite. *Spectrochimica Acta Part A: Molecular and Biomolecular Spectroscopy*, Vol. 117, pp. 158–162, https://doi.org/10.1016/j.saa.2013.08.014

Tanaka S., Hatano H., Itasaka O. (1960) Amino acid composition of conchiolin in pearl and shell. Biochemical studies on pearl. IX. *Journal of Biochemistry*, Vol. 33, No. 4, pp. 543–545, https://doi.org/10.1246/bcsj.33.543

Vaz N., Sturman N., Al-Alawi A. (2023) Gem News International: Microscopic shells in natural pearls from *Pinctada radiata*. *G&G*, Vol. 59, No. 1, pp. 143–145.

Wehrmeister U., Jacob D.E., Soldati A., Hofmeister W. (2007) Vaterite in freshwater cultured pearls from China and Japan. *Journal of Gemmology*, Vol. 31, No. 7, pp. 399–416.